Scientia Iranica F (2011) 18 (3), 765–771

Sharif University of Technology

Scientia Iranica

Transactions F: Nanotechnology

www.sciencedirect.com

Anti-scratch and adhesion properties of photo-curable polymer/clay nanocomposite coatings based on methacrylate monomers

Sh. Mohamadpour [a], B. Pourabbas [a,*], P. Fabbri [b]

[a] *Faculty of Polymer Engineering, Nanostructured Materials Research Center, Sahand University of Technology, Tabriz, P.O. Box 51335-1996, Iran*
[b] *Dipartimento di Ingegneria dei Materiali e dell'Ambiente, Università di Modena e Reggio Emilia, Via Vignolese 905A, 41100 Modena, Italy*

Received 5 December 2010; revised 23 January 2011; accepted 28 February 2011

KEYWORDS

Nanocomposite;
Coating;
Anti scratch;
Poly(methylmethacrylate);
Bis-GMA;
TEGDMA.

Abstract Different types of polymer/clay nanocomposite were prepared and evaluated for their application as hard and anti-scratch coating materials. Photo-curable nanocomposites, based on 2,2-bis[4-(methacryloxypropoxy)-phenyl]propane (Bis-GMA (2,2-bis[4-(methacryloxypropoxy)-phenyl]propane)) and tri (ethylene glycol)dimethacrylate (TEGDMA (tri(ethylene glycol)dimethacrylate)) (50/50 wt%) were prepared using three types of clay at different loading levels. The adhesion properties and scratch resistivity of the coatings on polymethymethacrylate slabs were investigated. The results were correlated with the clay dispersion state, determined by a transmission electron microscopy, X-ray diffraction and the surface morphology by atomic force microscopy. It was concluded that exfoliation or intercalation plays an important role, primarily in surface roughness, which in turn affects adhesion by changing the characteristics of the coating-substrate interface. The highest scratch resistivity with appropriate adhesion quality was obtained for a sample containing 1 wt% of more compatible clay, Cloisite® 30B in the nanocomposite resin mixture.

1. Introduction

Different types of plastic material are currently available for use as substitutes for mineral glass, owing to their superior properties, such as lightness, ease of mass production and lower price. Among them, poly(methylmethacrylate) (PMMA) and polycarbonate (PC) are two of the most well-known and widely used plastics with excellent optical properties [1]. However, one of the main disadvantages of the organic glasses is their weakness to scratch. Therefore, improving surface resistance against mechanically induced scratches, without any trade-off in transparency and optical properties, still remains a challenge in the field of organic glasses. Inorganic coatings applied by gas-phase or vacuum deposition are widely used to enhance scratch resistance. However, the drawbacks of these techniques are the high cost production process and the poor adhesion of the final coat to the substrate [2]. During the past decade, polymer/layered silicate (PLS (Polymer/layered silicate)) nanocomposites, comprised of one dispersed phase at the nanoscale, which is usually from layered clays, in a polymer matrix, have been emerged and studied in a wide range of research work. The effect of nanoscale layers has been recognized to enhance many properties of the pristine polymer, including mechanical and gas barrier properties, as well as flame retardancy [3–10]. Technically, clay minerals are used in the form of organic modified clays to fulfill the requirements for organic monomers or polymer chains to intercalate between the clay layers. Depending on the clay layer dispersion state, two major types of polymer/clay nanocomposite are supposed to generally occur. Exfoliation is when layers are individually dispersed and intercalated, and in which stacked layers of the clay are dispersed with polymer chains diffused between the galleries [11–13]. Among the variety of potential applications for PLS compounds, they have been noticed for their coating applications as well. One of the interesting applications of PLS nanocomposites as a coating material has been their ability to protect metallic surfaces from corrosion [14–16]. The primary effect of the nanoscale clay fillers in this application is to

* Corresponding author.
E-mail address: pourabas@sut.ac.ir (B. Pourabbas).

1026-3098 © 2011 Sharif University of Technology. Production and hosting by Elsevier B.V. Open access under CC BY-NC-ND license.
Peer review under responsibility of Sharif University of Technology.

doi:10.1016/j.scient.2011.06.001

Production and hosting by Elsevier

function as a physical barrier against aggressive species, such as O_2 and H^+, by a torturous pathway created by clay layers.

However, PLS nanocomposite coatings for hard and anti-scratch purposes have rarely been investigated [17,18]. Interesting results have recently been obtained by Fogelstrom et al., using a newly emerged class of PLS nanocomposites that utilizes hyperbranched polymers as the matrix [19]. They have examined the application of such hyperbranched polymer/clay nanocomposites, polyester Boltorn H30 [20] thermally cured with hexakis (methoxymethyl) melamine as a cross-linker, successfully, and obtained hard and flexible coating materials. Increased surface hardness, scratch resistance, flexibility and excellent chemical resistance, as well as adhesion, were obtained for the examined nanocomposite coatings [19].

Although thermally initiated polymerization and cross-linking reactions have been the most widely used method for various polymer/clay nanocomposite formations, their preparation by photo-polymerization methods, using UV irradiation, for example, has not been investigated widely [8,17,18,21]. UV curing technology carries advantages, such as being solvent-free, having low energy consumption and short processing time, which make the method favorable for many industrial applications including coating industries [22]. UV curable urethane–acrylate nanocomposites with synthetic layered silicates were investigated by Lv et al. for the coating application. Remarkable enhanced thermal and mechanical properties, compared to the pure polymer, were concluded even for an intercalated clay dispersion state [22]. On the other hand, matrix compounds mostly used for PLS materials with a coating application have been cross-linkable monomers (thermal or photo-curable) or resins such as epoxy, polyurethene or acrylate compounds. The superior mechanical properties have been the motivation for using highly cross-linkable matrixes in reinforced composite materials, with applications from structural to dental restorative composites. The latter composite utilizes acrylate based, highly cross-linkable monomers, which are made photocurable usually by a blue light. The mechanical properties of the final dental composites are comparable with flexural strength, dimensional tensile strength and the abrasion resistivity of the tooth [21,23].

In order to examine the capability of PLS nanocomposites with a matrix similar to that of dental composite resins, as a photo-curable hard and anti-scratch coating, the present work was planned. For the purpose of the work, highly cross-linkable UV-curable resin mixtures composed of 2,2-bis[4-(methacryloxypropoxy)-phenyl]propane (Bis-GMA) and tri (ethylene glycol)dimethacrylate (TEGDMA) were selected, which are exactly the same monomers used in common dental restorative composites. Bis-GMA has the advantages of low volatility and high tissue diffusivity, and forms high-modulus polymers with less volumetric shrinkage. However, Bis-GMA is a highly viscous fluid, thus, affording working and filler dispersion difficulties, as well as lower double bond conversion rates. To overcome the problem, a second thinner monomer, tri (ethylene glycol) dimethacrylate (TEGDMA), is usually added to Bis-GMA [23,24].

Coating precursors in the present study were prepared by a 50/50 (wt%) mixture of Bis-GMA/TEGDMA and loaded with different weight percentages of modified or unmodified clays. The PLS resins were then applied as a thin coating layer over PMMA (Poly(methylmethacrylate)) slabs as the substrate. The adhesion strength, scratch resistance, surface morphology and clay dispersion state of the coatings were investigated after curing by UV irradiation, using appropriate methods and instruments.

2. Materials and methods

2.1. Materials

Bis-GMA and TEGDMA monomers were purchased from Aldrich (USA) and used without further purification. The following fillers were used: organically modified montmorillonite Cloisite® 30B (Cs30B; cation exchange capacity 90 mequiv/100 g) modified by dihyroxyethyl octadecyle methyl ammonium chloride; Cloisite® 93A (Cs93A) modified by methylated dehydrogenated tallow ammonium; and sodium montmorillonite (Cloisite® Na^+). All fillers were obtained from Southern Clay (USA) and were used after dehydration at 80 °C for 24 h. The photo-polymerization initiator, suitable for UV wavelengths, was 2,2-dimethoxy-2-phenylacetophenone (Aldrich). The substrates were 3 mm thick PMMA slabs supplied by Aida Plastic Co. (Iran). These were cut into pieces of 5×5 ($cm \cdot cm$) and were washed thoroughly with detergent and distilled water before use.

2.2. Coating precursor preparation and coating process

Bis-GMA/TEGDMA (50/50 wt%) was prepared by mixing for 30 min. Then different amounts (1, 3, 5, 7 wt%) of the clay were added and mixed for 2 h. After mixing, the clays were dispersed by ultrasonication (20 kHz, 45–50 W) in an ice-water bath for 4 min. The UV initiator (0.5 wt%) was then added and applied to the substrate using a wire-wound applicator to prepare a wet coat layer. Samples were cured at a distance of 10 cm from an UV lamp (25 W, Philips, medium-pressure mercury) for 10 min. The final coating thickness was approximately 50 μm for all samples.

2.3. Characterization

Scratch resistance tests were performed using a CSM instrument equipped with an optical microscope and a Rockwell diamond micro-indenter of 200 mm in radius. Tests were carried out on a moving surface under the indenter for a scratch length of 3 mm and a load range from 100 mN to 20 N.

Transmission Electron Microscopy (TEM) images were obtained on a JEOL JEM 2010 instrument at an acceleration voltage of 200 kV. Specimens were prepared using a diamond knife ultramicrotome and then transferred to a 200-mesh carbon-coated copper grid.

Wide-angle X-Ray Diffraction (XRD) measurements were made using a rotating-anode X-ray generator (Siemens D 5000 diffractometer, 40 kV, 30 mA) with Cu K_α radiation ($\lambda = 0.154$ nm). The 2θ range 2°–15° was scanned at a speed of 0.02°/min.

Atomic Force Microscopy (AFM) measurements were carried out using a Park Autoprobe CP instrument. The DataPhysics OCA 20 system was used for contact angle measurements. To avoid surface contamination, all specimens were washed with THF (Tetrahydrofurane) and thoroughly dried just before measurement.

3. Results and discussion

3.1. Clay dispersion state in cured coatings

The encoding system and compositions of samples are summarized in Table 1. In order to evaluate the interlayer spacing of clay particles in the samples, diffraction peaks in XRD results were investigated, as shown in Figure 1. The original $CsNa^+$, Cs30B and Cs93A have an interlayer spacing of 11.7 Å, 18.5 Å and 23.6 Å, respectively.

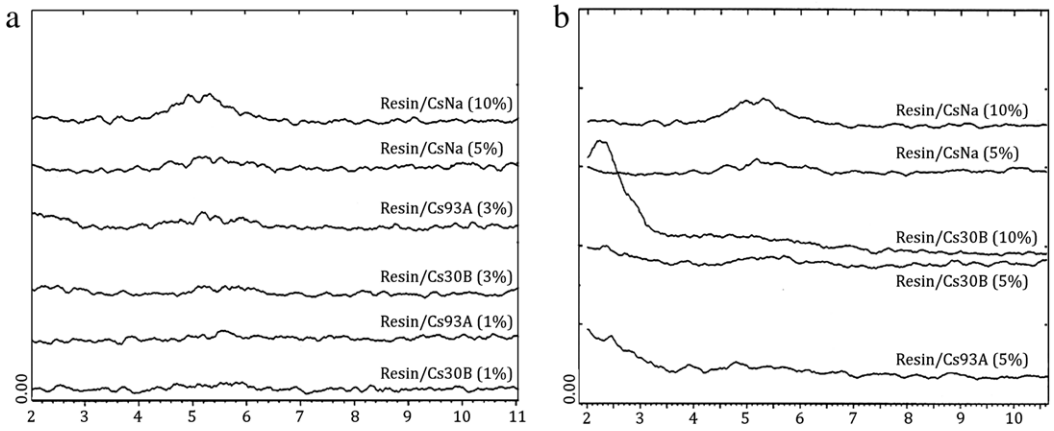

Figure 1: Wide angle X-ray diffraction patterns for different nanocomposite coatings after curing.

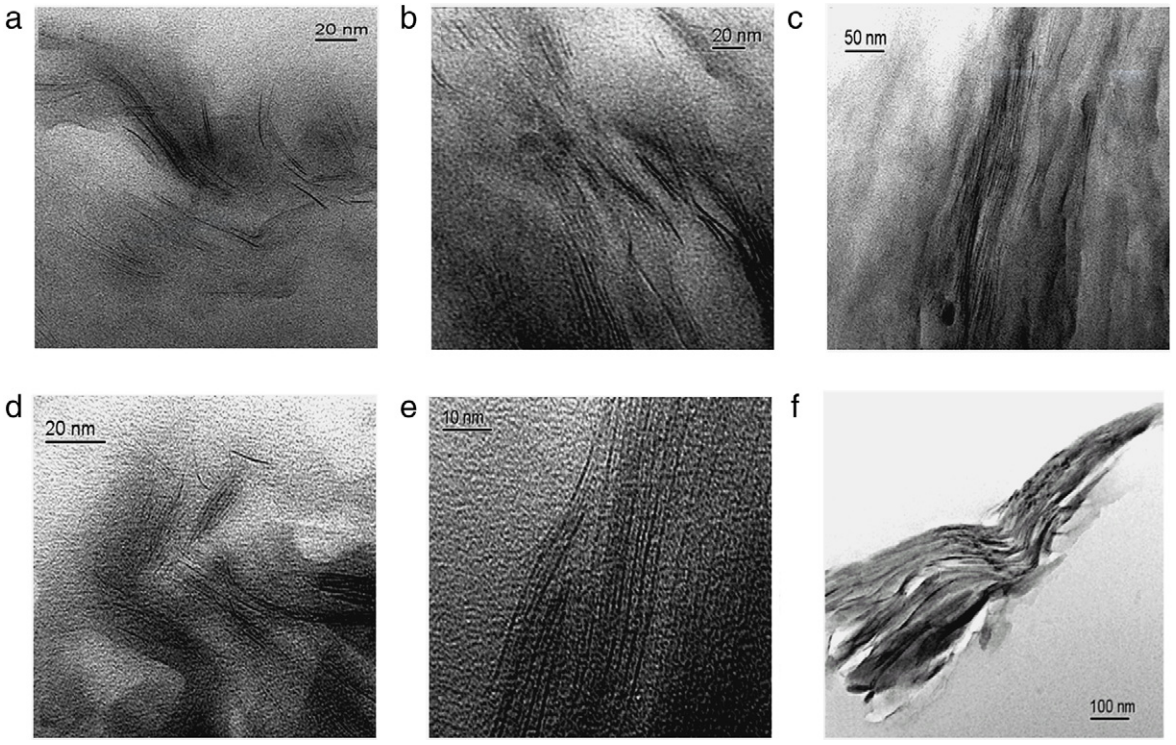

Figure 2: TEM micrographs showing: (a) resin/Cs30B (1%); (b) resin/Cs30B (3%); (c) resin/Cs30B (5%); (d) resin/Cs93A (1%); (e) resin/Cs93A (5%); (f) resin/$CsNa^+$ (5%).

Table 1: Coding and composition of different coatings used in this work.

Coatings	Clay used	X = wt% of filler			
Resin/Cs30B (X%)	Cloisite 30B	1	3	5	7
Resin/Cs93A (X%)	Cloisite 30B	1	3	5	7
Resin/$CsNa^+$ (X%)	CloisiteNa^+	1	3	5	7
Pure resin[a]	None	–	–	–	–

[a] Pure resin denotes to the 50/50 (wt%) mixture of Bis-GMA/TEGDMA with 0.5 wt% of photo-initiator.

As can be seen, there are no resolvable peaks on the 2θ scale for coatings containing Cs30B and Cs93A at 1 and 3 wt%. This indicates a possible exfoliated state for the clay layers within the matrix. At 5 and 10 wt% of Cs30B and Cs93A, an intercalation peak, especially for resin/Cs30B/10%, is appeared at the lower end of the 2θ scale, confirming the intercalated state. However, for samples containing $CsNa^+$, the XRD patterns in Figure 1(a) and (b) exhibit a wide diffraction peak around 5.5° (equal to 16.0 Å) in 2θ axis, especially for 10 wt% clay. This suggests the weak intercalation of the polymeric matrix within $CSNa^+$ layers, due to the incompatibility of unmodified clay with the organic matrix. In general, displacement of the diffraction peaks in PLS nanocomposites, with respect to the original clay, can be regarded as evidence for intercalation, if the size of the stacked layers is large enough (according to the Scherrer equation). Therefore, no decisive decision can be made between a real exfoliation and intercalation state by using only XRD results.

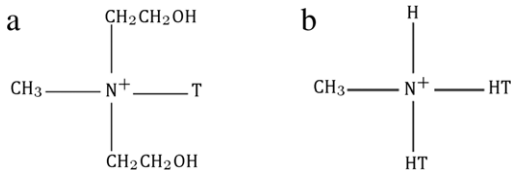

Figure 3: Molecule structure of the modifier cations used in (a) Cs30B (methyl tallow bis-2-ydroxyethyl quaternary ammonium) and (b) Cs93A (methyl dehydrogenated tallow quaternary ammonium).

However, complementary evidence by TEM can help in the final conclusion.

TEM images are shown in Figure 2 for different nanocomposites. Figure 2(a) confirms XRD results, regarding an exfoliated state for resin/Cs30B/1%, with individual layers detectable as dark lines. However, comparison of the TEM images in Figure 2(a)–(d) reveals gradual changes from an exfoliation to an intercalated state induced by increasing clay content. In the meantime, the size of intercalated zones increases with increasing clay content. On the other hand, comparison reveals better compatibility for Cs30B and the matrix compared to Cs93A, as the fraction of exfoliated layers is increased and the size of the intercalated zones is smaller in comparative samples for the former clay. The observed compatibility for Cs30B may be related to its modifier structure with two polar hydroxyl groups, which make it more of a polar cation, instead of non polar groups in Cs93A, as shown in Figure 3. Finally, Figure 2(f) confirms the XRD results for $CsNa^+$ containing nanocomposites, with a minimum clay/matrix interaction, and a large clay particle appeared in the TEM image.

3.2. Coating adhesion

Figure 4 compares optical micrographs of scratch test results for different coatings and the uncoated PMMA substrate. The trace of the indenter along its 3-mm path with varying force shows the different adhesion quality of the coatings. Coating adhesion can be evaluated in terms of the force at which the coating layer detaches from the substrate surface (PMMA), or serious destruction occurs for the coat layer. No detectable failure was observed for clay free coating (pure resin), suggesting a high quality adhesion to PMMA. The same result was also obtained for resin/Cs30B/1%, so that the coating layer resided all along the indentation groove without any detachment or destruction. However, coatings in sample resin/Cs30B/3% and resin/Cs30B/5% showed complete detachment at 8.7 N and 10.2 N, respectively, showing relatively poor adhesion quality for these samples. Therefore, it seems that lower clay content favors adhesion. However, good adhesion was retrieved at higher Cs30B content for resin/Cs30B/7%, without any failure during the scratch test (Figure 4(a)).

In contrast to Cs30B coatings, none of the Cs93A-containing nanocomposites exhibited an acceptable level of adhesion, as can be seen in Figure 4(b). However, on the other hand, excellent adhesion was observed for coatings containing $CsNa^+$ (Figure 4(c)). The phenomenology and possible reasons for the diverse adhesion quality observed in different samples are related to the clay content and type affecting the dispersion state of the clay layers, as discussed in subsequent sections.

3.3. Surface morphology by AFM

Previous results revealed that clay content and type can significantly influence coating adhesion. Since adhesion is directly

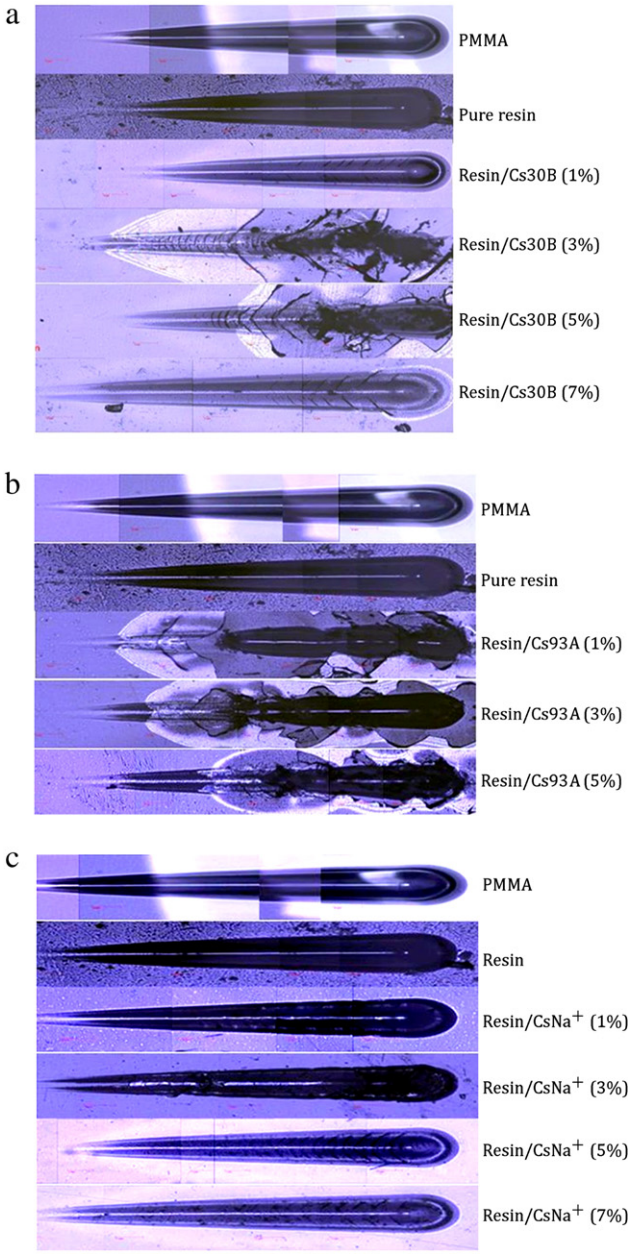

Figure 4: Optical micrograph of the scratch test results carried out on coated samples with different coating compositions as well as uncoated PMMA.

related to the quality of the coating-substrate interface, the effect of clay type and loading on the dispersion state of the clay inside the matrix was investigated. However, due to it being practically impossible to investigate the exact coating-substrate interface directly, i.e. tools such as electron microscopy can represent the interface only on fractured samples, the surface of the coating was examined using AFM, assuming that the clay-induced morphology on the surface is equivalent to that of the coating-substrate interface. The observation that clay particles do not precipitate from the coating precursors, even after 24 h or during curing, provided support for the assumption. Figure 5 shows phase separation and topographic AFM images for resin/Cs30B/5%, resin/Cs93A/5%, resin/$CsNa^+$/5% and resin/$CsNa^+$/10%. An increased surface roughness from resin/Cs30B/5% to resin/Cs93A/5% was observed, while sample

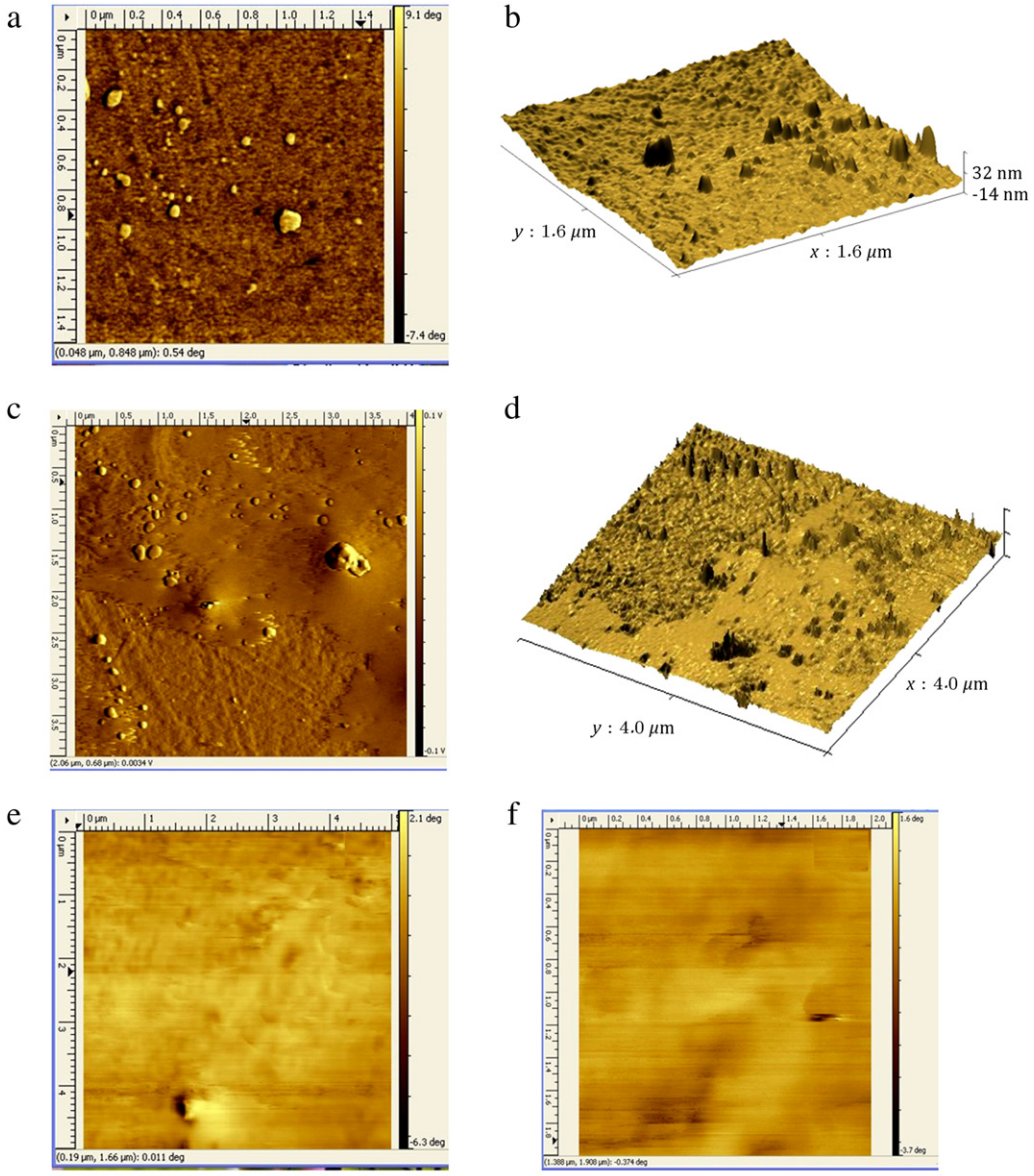

Figure 5: AFM images showing phase separation and surface topography of resin/Cs30B (5%) (a and b); resin/Cs93A (5%) (c and d) and phase separation images of resin/$CsNa^+$ (3%) and resin/$CsNa^+$ (5%) (e and f).

resin/$CsNa^+$/5% and resin/$CsNa^+$/10% showed very smooth surfaces. Therefore, it can be concluded that exfoliated layers, as already shown by TEM images, result in lower surface roughness. Conversely, intercalated particles increase surface roughness. This is in accordance with results reported by Decker et al. [9]. On the other hand, comparison of the perfect adhesion observed in the scratch test for PMMA samples coated with pure resin (Figure 4), compared with other samples coated by clay nanocomposites, provides further proof for the clay-induced roughness effect on adhesion quality. Increased roughness lowers the contact area between the coating and the substrate and, thus, reduces the adhesion performance. However, the very smooth surface obtained for coatings containing $CsNa^+$ (Figure 5) indicates that unmodified clay does not change the surface roughness because of the absence of exfoliation or effective intercalation. This led to the observed better adhesion quality of the coatings having unmodified clay (Figure 4(c)). Unmodified clay particles possibly agglomerate in the bulk of the material of the coating, and leave the pure resin to remain in effective contact with the substrate. Similar reasoning can also be used to explain the adhesion quality observed for resin/Cs30B/7%, with lower clay-matrix interaction owing to higher clay content.

3.4. Scratch resistance

Much information about the coating, including penetration depth, residual depth, acoustic wave emission and friction force, as a function of the applied load, are obtainable simultaneously in a single scratch test. However, residual depth provides criteria of how the coating resists mechanical scratch. Figure 6 compares the residual depth versus the applied load for uncoated PMMA and PMMA coated with pure resin, as well as resin/Cs30B and resin/Cs93A coated with nanocomposites having different clay content. As seen, the increase in residual depth by applied force (slope of the curve) depends on the

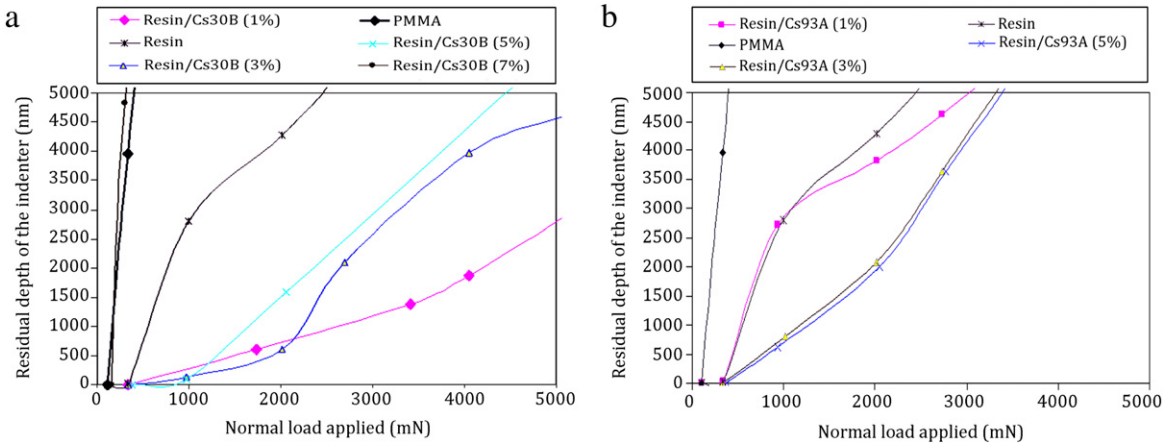

Figure 6: Residual depth–normal load variation obtained in scratch tests for (a) resin/Cs30B and (b) resin/Cs93A nanocomposite coatings having different clay content. The results for uncoated PMMA and coated with pure resin are provided also for comparison.

coating and the clay content. Uncoated PMMA and PMMA coated with pure resin show very weak scratch resistance, as reflected by a sharp increase in residual depth at low applied loads (Figure 6). However, resin/Cs30B/1% shows a very slow increase in residual depth, with applied loads >2000 mN (Figure 6(a)), which is the lowest slope observed among the series. This indicates the superior scratch resistance of this sample compared to bare PMMA and all other samples. Closer inspection of the curves at loadings <1000 mN reveals a relatively lower slope for resin/Cs30B/3% and resin/Cs30B/5%, than for resin/Cs30B/1%. However, the increased penetration depth and dramatic change in slope observed for the two former samples, after certain applied loads (900 and 2000 mN), happens due to the coating failure mechanisms of the coat layers including delamination, detachment and destruction. The total mechanical failure at lower applied forces is better resolved on visual inspection of the scratch test results, which have already been provided in Figure 4(a). It can be concluded that lower adhesion properties attributed to the clay dispersion effect, as discussed in the preceding section, scarify the initial enhanced scratch resistivity of the coating at higher and critical applied forces.

On the other hand, Figure 6(b) reveals a lack of any significant improvement in scratch resistivity for coatings containing Cs93A. A moderately higher rate of increase in residual depth, with applied force being almost independent of clay content, was observed for all Cs93A containing nanocomposite coatings. These samples also exhibited poor adhesion quality, as discussed in earlier sections.

Figure 7 compares the variation in residual depth as a function of applied load for PMMA slabs coated with $CsNa^+$-containing nanocomposite coatings. No significant improvement in scratch resistance, compared to pure resin, was observed, while they have shown good adhesion properties, as discussed previously (Figure 4(c)).

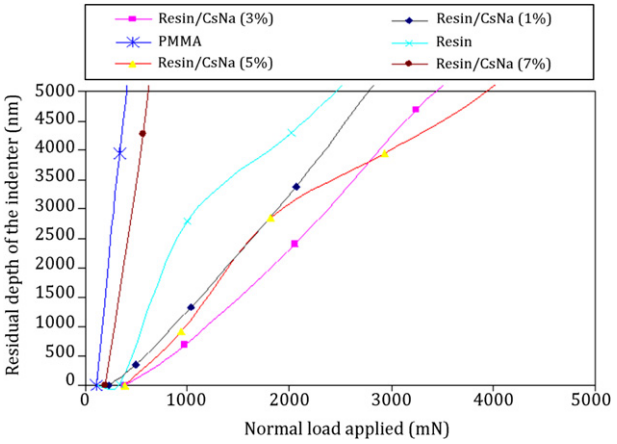

Figure 7: Residual depth–normal load variation obtained in scratch tests for resin/$CsNa^+$ with varying clay content compared to uncoated PMMA and coated with pure resin.

4. Conclusions

Polymer/clay nanocomposites can be used as photo-curable coatings to improve the surface mechanical properties of other materials, such as PMMA. Highly cross-linkable monomers or their mixtures can successfully be employed for the matrix of such nanocomposites, and yield hard enough materials, with a promising application as anti-scratch coating. It was observed that coating properties, in terms of scratch resistivity and adhesion, are highly dependent on the dispersion state of clay layers inside the resin mixture. This, in turn, let us say exfoliated or intercalated, depends on the clay loading level, as well as its compatibility with the resin mixture. Lower clay content favors exfoliation; however, intercalation is the predominant layer dispersion state as the clay content increases. A combination of factors influences the adhesion quality of the nanocomposite coatings to the substrate surface. Clay may increase surface roughness by increasing the clay content in the composition. Clay induced roughness can affect the coating-substrate interface, leading to a change in adhesion. A poorer adhesion property was observed for coatings with intercalated clay layers, while exfoliation was observed to enhance adhesion properties. On the other hand, unmodified clay does not change the surface roughness of the coating effectively, so that relatively good adhesion was observed for such coatings. Presumably unmodified clay particles agglomerate mainly inside the bulk, without any immigration to the surface or interface regions. The trend in scratch resistance improvement of the coatings was observed to be in an opposite direction to adhesion. The optimum point coincided at the nanocomposite coating with very low content (1 wt%) of the more compatible clay, Cloisite® 30B.

References

[1] Tanglumlert, W., Prasassarakich, P., Supaphol, P. and Wongkasemjit, S. "Hard-coating materials for poly (methyl methacrylate) from glycidoxypropyltrimethoxysilane-modified silatrane via a sol–gel process", *Surface & Coatings Technology*, 200, pp. 2784–2790 (2006).

[2] Messori, M., Toselli, M., Pilati, F., Fabbri, E., Fabbri, P. and Busoli, S. "Poly (caprolactone)/silica organic–inorganic hybrids as protective coatings for poly (methyl methacrylate) substrates", *Surface Coatings International Part B—Coatings Transactions*, 86, pp. 181–186 (2003).

[3] Krook, M., Albertsson, A.C., Gedde, U.W. and Hedenqvist, M.S. "Barrier and mechanical properties of montmorillonite/polyesterarnide nanocomposites", *Polymer Engineering and Science*, 42, pp. 1238–1246 (2002).

[4] Tong, Z.H. and Deng, Y.L. "Synthesis of water-based polystyrene–nanoclay composite suspension via miniemulsion polymerization", *Industrial & Engineering Chemistry Research*, 45, pp. 2641–2645 (2006).

[5] Yeh, J.M., Liou, S.J., Lai, M.C., Chang, Y.W., Huang, C.Y., Chen, C.P., Jaw, J.H., Tsai, T.Y. and Yu, Y.H. "Comparative studies of the properties of poly (methyl methacrylate)-clay nanocomposite materials prepared by in situ emulsion polymerization and solution dispersion", *Journal of Applied Polymer Science*, 94, pp. 1936–1946 (2004).

[6] Sun, Q.H., Schork, F.J. and Deng, Y.L. "Water-based polymer/clay nanocomposite suspension for improving water and moisture barrier in coating", *Composites Science and Technology*, 67, pp. 1823–1829 (2007).

[7] Di Gianni, A., Amerio, E., Monticelli, O. and Bongiovanni, R. "Preparation of polymer/clay mineral nanocomposites via dispersion of silylated montmorillonite in a UV curable epoxy matrix", *Applied Clay Science*, 42, pp. 116–124 (2008).

[8] Fogelstrom, L., Antoni, P., Malmstrom, E. and Hult, A. "UV-curable hyperbranched nanocomposite coatings", *Progress in Organic Coatings*, 55, pp. 284–290 (2006).

[9] Decker, C., Keller, L., Zahouily, K. and Benfarhi, S. "Synthesis of nanocomposite polymers by UV-radiation curing", *Polymer*, 46, pp. 6640–6648 (2005).

[10] Burgentzle, D., Duchet, J., Gerard, J.F., Jupin, A. and Fillon, B. "Solvent-based nanocomposite coatings, I. Dispersion of organophilic montmorillonite in organic solvents", *Journal of Colloid and Interface Science*, 278, pp. 26–39 (2004).

[11] Ishida, H., Campbell, S. and Blackwell, J. "General approach to nanocomposite preparation", *Chemistry of Materials*, 12, pp. 1260–1267 (2000).

[12] Priya, L. and Jog, J.P. "Poly (vinylidene fluoride)/clay nanocomposites prepared by melt intercalation: crystallization and dynamic mechanical behavior studies", *Journal of Polymer Science Part B—Polymer Physics*, 40, pp. 1682–1689 (2002).

[13] Yu, Y.H., Yeh, J.M., Liou, S.J. and Chang, Y.P. "Organo-soluble polyimide (TBAPP-OPDA)/clay nanocomposite materials with advanced anticorrosive properties prepared from solution dispersion technique", *Acta Materiala*, 52, pp. 475–486 (2004).

[14] Yeh, J.M. and Chang, K.C. "Polymer/layered silicate nanocomposite anticorrosive coatings", *Journal of Industrial and Engineering Chemistry*, 14, pp. 275–291 (2008).

[15] Chang, K.C., Chen, S.T., Lin, H.F., Lin, C.Y., Huang, H.H., Yeh, J.M. and Yu, Y.H. "Effect of clay on the corrosion protection efficiency of PMMA/Na+-MMT clay nanocomposite coatings evaluated by electrochemical measurements", *European Polymer Journal*, 44, pp. 13–23 (2008).

[16] Nematollahi, M., Heidarian, M., Peikari, M., Kassiriha, S.M., Arianpouya, N. and Esmaeilpour, M. "Comparison between the effect of nanoglass flake and montmorillonite organoclay on corrosion performance of epoxy coating", *Corrosion Science*, 52, pp. 1809–1817 (2010).

[17] Ceccia, S., Turcato, E.A., Maffettone, P.L. and Bongiovanni, R. "Nanocomposite UV-cured coatings: organoclay intercalation by an epoxy resin", *Progress in Organic Coatings*, 63, pp. 110–115 (2008).

[18] Li, F.S., Zhou, S.X., Gu, G.X., You, B. and Wu, L.M. "Preparation and characterization of ultraviolet-curable nanocomposite coatings initiated by benzophenone/*n*-methyl diethanolamine", *Journal of Applied Polymer Science*, 96, pp. 912–918 (2005).

[19] Fogelstrom, L., Malmstrom, E., Johansson, M. and Hult, A. "Hard and flexible nanocomposite coatings using nanoclay-filled hyperbranched polymers", *ACS Applied Materials and Interfaces*, 2, pp. 1679–1684 (2010).

[20] Malmstrom, E., Johansson, M. and Hult, A. "Hyperbranched aliphatic polyesters", *Macromolecules*, 28, pp. 1698–1703 (1995).

[21] Mahmoodian, M., Pourabbas, B. and Arya, A.B. "Preparation and characterization of Bis-GMA/TEGDMA/clay nanocomposites at low filler content regimes", *Journal of Composite Materials*, 44, pp. 1379–1395 (2010).

[22] Lv, S.C., Zhou, W., Miao, H. and Shi, W.F. "Preparation and properties of polymer/LDH nanocomposite used for UV curing coatings", *Progress in Organic Coatings*, 65, pp. 450–456 (2009).

[23] Mahmoodian, M., Arya, A.B. and Pourabbas, B. "Synthesis of organic–inorganic hybrid compounds based on Bis-GMA and its sol–gel behavior analysis using Taguchi method", *Dental Materials*, 24, pp. 514–521 (2008).

[24] Reed, B.B., Choi, K., Dickens, S.H. and Stansbury, J.W. "Effect of resin composition on kinetics of dimethacrylate photopolymerization", *Abstracts of Papers of the American Chemical Society*, 214, p. 41-Poly (1997).

Shahram Mohammadpour, joined the Faculty of Chemical Engineering in Sahand University of Technology as an M.S. Degree student in 2005. He received his M.S. Degree in Nanostructured Materials Engineering in 2007. His thesis title was Anti-Scratch Coatings Based on Polymer/Clay Nanocomposites. He pursued his research at Sahand University of Technology and the University of Modena and Reggio Emilia, in Modena, Italy. He is now doing his Ph.D. at the University of Modena, Italy, under the supervision of Dr. Paola Fabbri.

Behzad Pourabbas, the corresponding author, is currently Professor at the Polymer Engineering Faculty at Sahand University of Technology, Tabriz, Iran. He received his Ph.D. Degree from Shiraz University in 1996 and joined the faculty of Chemical Engineering immediately as Assistant Professor.

He is the author of several papers in the field of nanostructured materials including Nanocomposites, Nanoparticles, Nanocatalysists, etc. His current research fields include Surface Modification of Nanoparticles and Polymeric Materials, Nano-Micro Imprinting and Particulate Reinforced Polymeric Materials.

Paola Fabbri is Academic Fellow and Assistant Professor at the Materials and Environmental Engineering Department in the University of Modena and Reggio Emilia, Modena, Italy. She has been the author of several journal papers, mainly on the Coatings of Polymeric Substrates for Anti-Scratch, Hydrophobicity, Anti-Bacterial and other purposes. She is the member of a research group supervised by Professor Francesco Pilati, one of the pioneering groups on the field of coating technology from scientific point of view as well as research equipments.